Data-Driven Prediction of Damage Distribution in Prepreg Platelet Molded Composites from Coarse Structural Descriptors

K. Çelebi*, S.G. Kravchenko

Department of Materials Engineering, The University of British Columbia, Vancouver, Canada

* *Corresponding author (kuthan.celebi@ubc.ca)*

Keywords: *Prepreg platelet molded composites; Damage distribution; Multiscale Modeling; Deep Learning*

1. Abstract

This study investigates whether coarse structural descriptors can provide sufficient information for predicting spatial distribution of damage intensity in Prepreg Platelet Molded Composites (PPMCs) with a spatially heterogenous stochastic mesostructure. Coarse structural descriptors are defined as through-thickness averaged descriptions of mesoscale fiber orientation distribution (FOD) expressed using spatial heatmaps of second-order orientation tensor components. A synthetic dataset is generated using a previously developed finite element progressive failure framework with explicitly represented platelet-level mesostructure. A gradually increasing number of layerwise orientation tensor fields are homogenized through the thickness to produce structural representations at multiple resolution levels, which are subsequently used to train U-Net surrogate models for predicting post-peak front- and back-face damage distribution maps. The surrogate predictions successfully reproduce major damage patterns and distributed damage behavior observed in the ground truth simulations. Reductions in structural representation resolution lead to a gradual decrease in predictive accuracy with mean absolute percentage error on pixelwise damage intensity prediction increasing from approximately 5% to 9%. Overall, the results suggest that accessible, coarse structural descriptors can be used for data-driven analysis of damage distribution in composites with a stochastic mesostructure such as PPMCs.

2. Introduction

Prepreg Platelet Molded Composites (PPMCs) are long discontinuous fiber-reinforced composites that are suitable for diverse structural applications due to their combination of processability and mechanical performance. The mesostructure of PPMC parts comprise platelets of unidirectional prepreg tape that are randomly distributed and compression molded, resulting in a complex, overlapping arrangement with uncontrolled orientations as seen in Fig. 1a-b. This process-induced stochastic mesostructure unique to each component leads to a pronounced variability in the nonlinear mechanical response and failure location of PPMCs. Additionally, the damage process zone in PPMCs is inherently dispersed (Fig. 1c), with multiple competing damage sites developing at various locations within each part.

The progressive failure behavior and damage distribution of PPMC mechanical properties have been successfully modeled via Direct Computational Homogenization methods that explicitly represent the arrangement of platelets [1-3]. However, resolving fine structural details such as orientations of individual platelets are experimentally and computationally demanding across large volumes [4-6]. Hence it is worth investigating the potential for analyzing the damage distribution of PPMCs using accessible, coarse structural descriptors via alternative modeling methods.

Data-driven surrogate models utilizing machine learning tools have recently been utilized in analyzing upscale properties or full-field stress distributions from micro-RVE images [7-11]. Convolutional neural networks (CNNs) with encoder-decoder architectures such as U-Nets emerge as an especially suitable class of models due to their ability to learn spatially correlated features from image-based representations and predict finely resolved output features accurately. However, existing surrogate approaches often highlight relative gains in computational efficiency while preserving the structural detail requirements of the numerical models generating their training data. The framework of this study expands on this existing approach by focusing on the capability of data-driven surrogates to infer spatial damage distributions from coarse structural data. A physics-based synthetic tensile test dataset is generated via a previously developed finite element (FE) progressive failure model with explicitly represented mesostructure. The available fiber orientation distribution (FOD) data from the virtual samples are then averaged through-the-thickness to train a U-Net surrogate model to map these deliberately coarsened structural inputs to damage maps at the post-peak stress regime. Various resolution levels of input structural data are tested to study their relative effects on predictive performance.

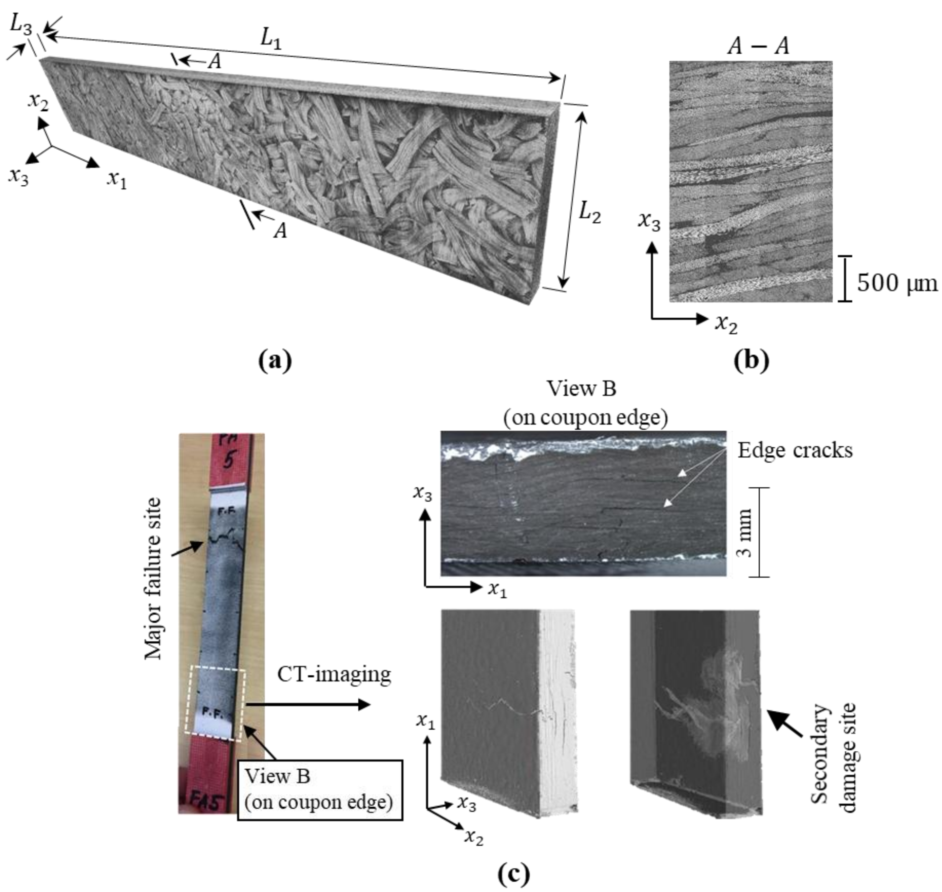

Figure 1. PPMC mesostructure and damage dispersion

3. Methodology

3.1. Synthetic Dataset Generation

A synthetic dataset of tensile test simulations is generated using a previously developed FE-based progressive failure analysis (PFA) framework with PPMC mesostructure represented explicitly at the platelet-level (Fig. 2a). A coupon domain $\Omega \subset \mathrm{R}^3$ with dimensions $L_1 \times L_2 \times L_3 = 152.4 \times 25.4 \times 1.2mm^3$ is filled with platelets of size $25.4 \times 12.7 \times 0.12mm^3$ via a sequential adsorption procedure in DIGIMAT [12], designating the centroid location and in-plane orientation of each platelet by sampling a uniform random distribution. A local material coordinate system $(p_i q_i r_i)$ is defined for each platelet, where the local fiber alignment is determined by the orientation of the local axes relative to the global coordinate system. The resulting morphology is discretized into voxels and each voxel is appointed to a single platelet. The voxelized model is then imported into ABAQUS/Standard [13] to simulate progressive failure under uniaxial tensile loading.

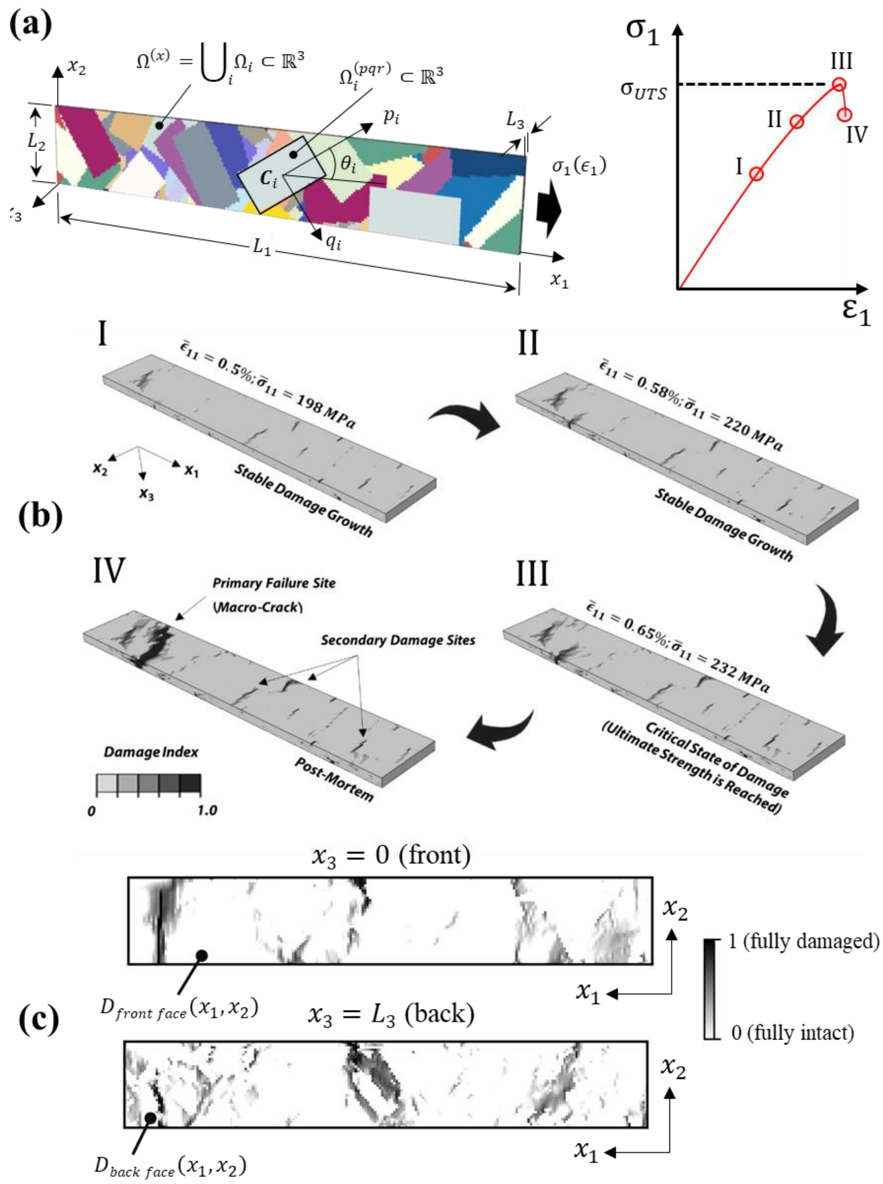

Figure 2. Progressive failure analysis of a PPMC and the post-peak damage distribution heatmaps used as a ground truth output for data-driven surrogate modelling.

Damage evolution under tensile loading is simulated using the progressive failure framework of [14] combining continuum damage mechanics and cohesive zone modeling approaches. Representative stages of damage evolution throughout the loading history are illustrated in Fig. 2b. The simulated damage process is characterized by the progressive formation of multiple competing damage sites, followed by localized damage growth and eventual macroscopic failure. For each virtual coupon, front and back-face damage maps are extracted at a post-peak loading stage corresponding to a 10% reduction in global stress from the peak stress value. The extracted damage maps represent the local remaining load-carrying capability and serve as the ground truth outputs for surrogate model training. Representative examples of the resulting ground truth outputs for the surrogate model in the form of damage distribution heatmap images are shown in Fig. 2c.

3.2. *Reduced-Resolution Structural Representations*

The surrogate model inputs are generated via a multi-step transformation of the FE mesostructure model. The explicitly represented mesostructure is first described as the collection of layerwise distributions of the in-plane angle θ as expressed in Fig. 3a and the second-order orientation tensor components a_{11} and a_{12} are then calculated following [15]. Subsequently, the a_{11}, a_{12} values at each voxel are locally averaged through-the-thickness across Z neighboring layers as expressed in Eqn. 1 to produce a deliberately coarsened description.

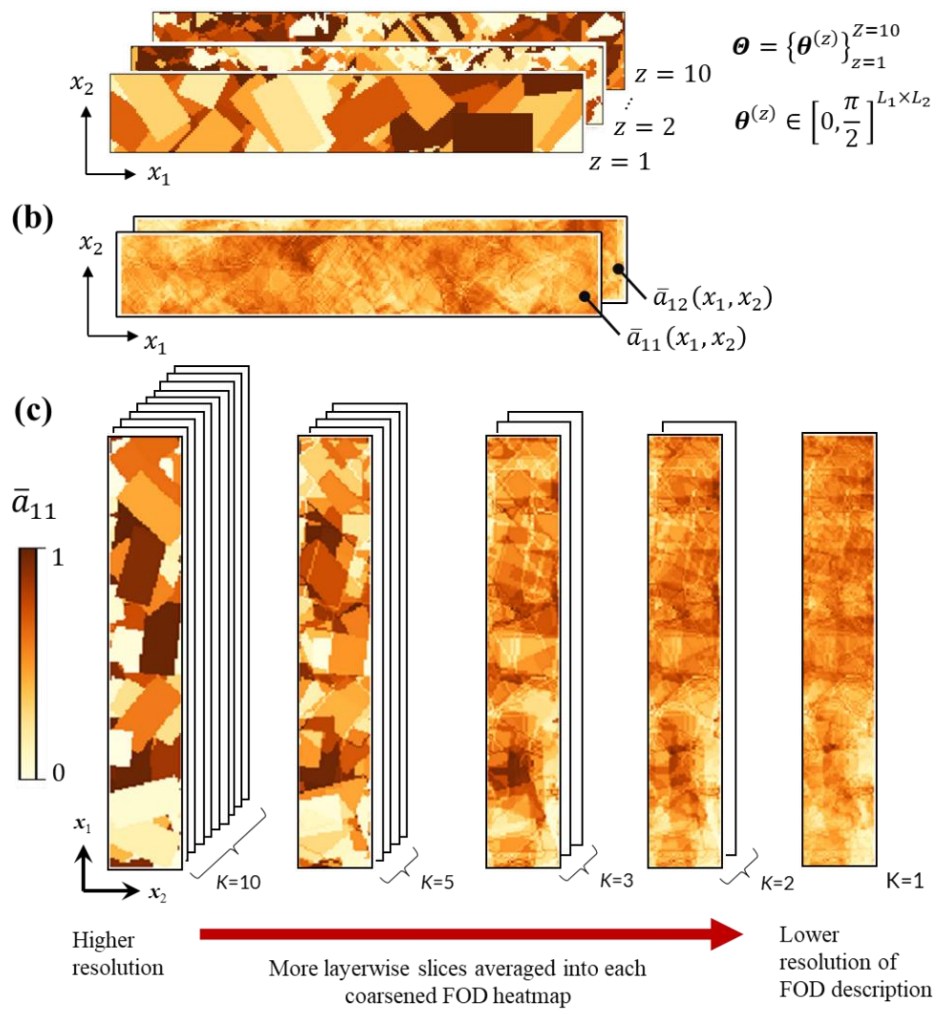

Figure 3. Reduced-resolution structural representation of a PPMC.

The number of neighboring voxels that are averaged through the thickness (Z) and homogenized into a single value determines the total number of unique a_{11}, a_{12} values (K) through the thickness. For example, the a_{11}, a_{12} data from 10 total voxels through the thickness can be averaged into K=5 independent values if the values from Z=10/K= 2 neighboring voxels are averaged together for each independent coarsened (i.e. through-thickness averaged) $\bar{a}_{1j}$ heatmap. If Z=1 (i.e. K=10), no resolution reduction will occur and layerwise values will be preserved as is, while if Z=10 and K=1, the a_{11}, a_{12} are fully homogenized through-the-thickness as shown in Fig. 3b. In-plane heterogeneity is fully preserved in all cases. The total number of independent orientation states through the coupon thickness at any location in-plane (K) is considered as a critical hyperparameter and separate surrogate models are trained using K=1,2,3,5,10 as inputs as shown in Fig. 3c to study the effect of using structural representations at various resolutions. The surrogate model input tensor X is expressed in Eqn. 2 where H and W denote the number of pixels along the coupon length and width respectively.

$$\bar{a}_{1j}(x_1, x_2) = \frac{1}{Z}\sum_{z=1}^{Z} a_{1j}^{(z)}(x_1, x_2), \qquad j \in \{1,2\} \tag{1}$$

$$X = \bar{\boldsymbol{A}}_{1j} = \left\{\bar{a}_{1j}^{(k)}(x_1, x_2)\right\}_{k=1}^{K}, \qquad \begin{array}{l} j = 1,2 \\ \bar{\boldsymbol{A}}_{11}, \bar{\boldsymbol{A}}_{12} \in \mathbb{R}^{K \times H \times W} \end{array} \tag{2}$$

3.3. Data-Driven Surrogate Modeling Framework

A four-layer U-Net model with the architecture illustrated in Fig. 4 is employed to learn a mapping between the reduced-resolution structural representations and the damage distribution heatmap images. Input heatmaps were padded to dimensions compatible with repeated downsampling operations within the network architecture. Separate surrogate models were trained for each structural representation resolution level (K=1,2,3,5,10). The dataset was divided into subsets for training (70%), validation (15%), and testing (15%). Model training was performed using the Adam optimizer and a SmoothL1 loss function.

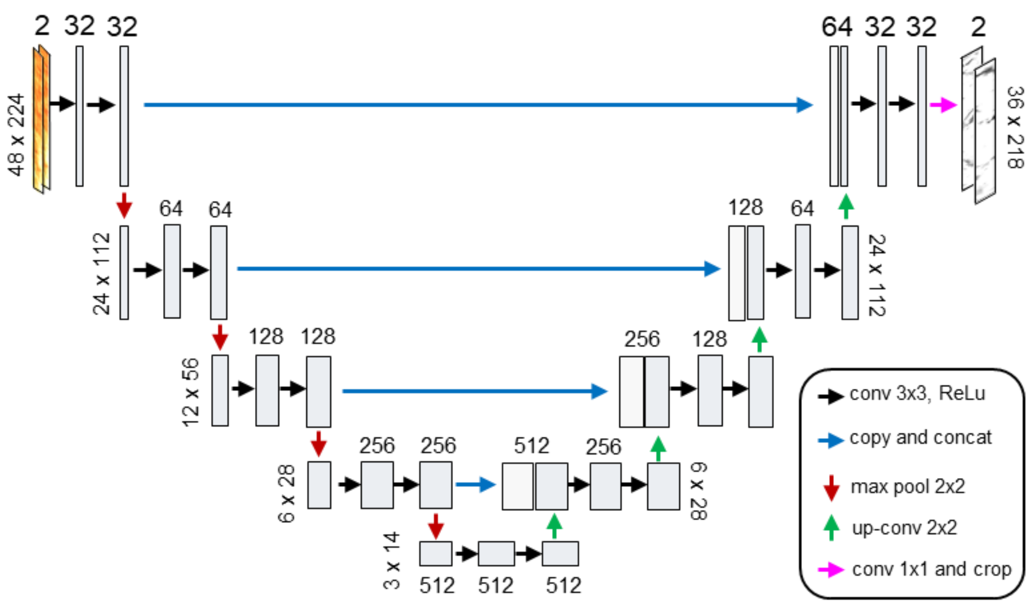

Figure 4. Surrogate U-Net model with coarsened inputs (K=1)

4. Results and Discussion

Representative predicted damage distribution heatmaps obtained using surrogate models trained with different structural representation resolutions are shown in Fig. 5. The results demonstrate that the proposed surrogate modeling framework is capable of reproducing major spatial damage localization trends and distributed damage behavior from reduced-resolution structural descriptors. The predicted damage maps generally capture the primary high-damage regions observed in the ground truth outputs while also reproducing broader distributed damage patterns throughout the specimen geometry. The influence of structural representation resolution on prediction capability is evident in both the qualitative comparisons of Fig. 5 and the quantitative performance metrics Mean Absolute Error (MAE), Root Mean Squared Error (RMSE) and Normalized Cross Correlation (NCC) summarized in Table 1.

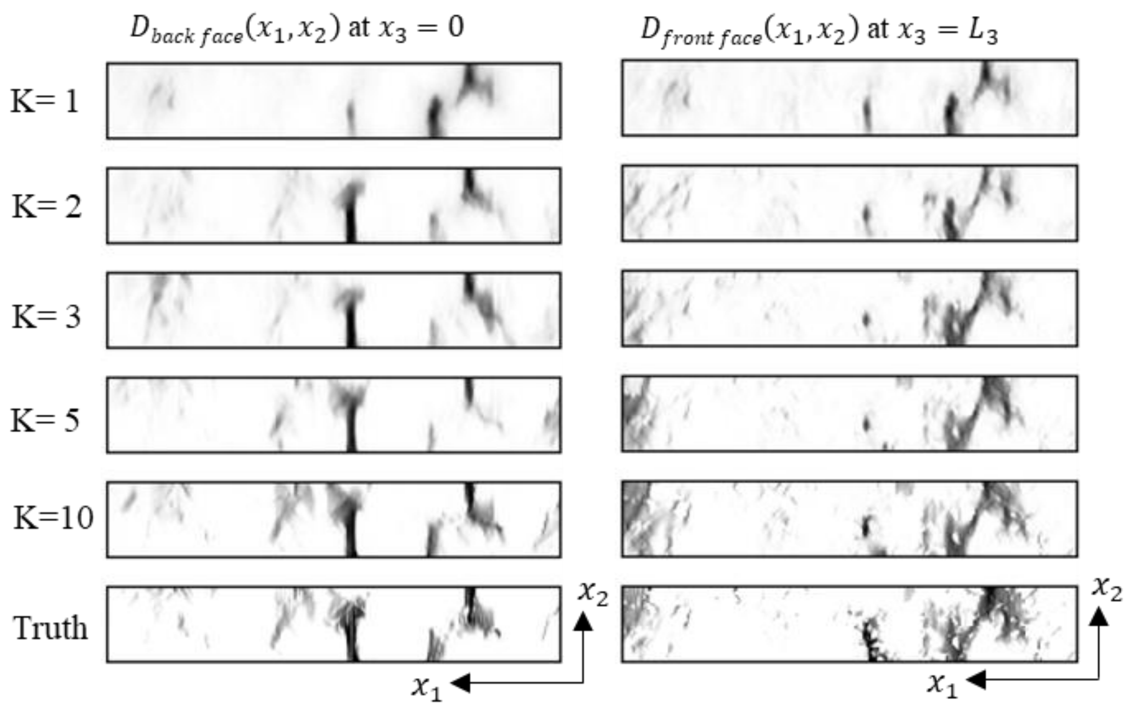

Figure 5. Predicted damage maps at various input structural resolutions (top) vs the ground truth (bottom)

Increasing structural representation resolution improves prediction quality, with higher-resolution inputs producing sharper and more localized damage patterns that more closely resemble the ground truth outputs. Nevertheless, despite the reduction in structural information available to the lower-resolution models with coarsened input images, the predicted maps still successfully identify major damage regions. This observation suggests that reduced mesoscale structural descriptors retain meaningful information relevant to macroscopic damage evolution in PPMCs. The quantitative metrics presented in Table 1 show consistent improvement in MAE, RMSE, and NCC values with increasing structural representation resolution. The K=10 model produces the best overall agreement with the ground truth damage maps across the evaluated metrics, with a mean absolute error of approximately 5% on pixelwise prediction of damage intensity.

Table 1. Performance metrics for surrogate models trained with different input resolutions

K hyperparameter	MAE	RMSE	NCC
1	0.091	0.178	0.479
2	0.074	0.152	0.647
3	0.068	0.144	0.694
5	0.061	0.130	0.754
10	0.054	0.121	0.796

While MAE and RMSE metrics depend on the mean error in predicted damage intensity at every local pixel location across all samples in the test dataset, the NCC is a standard metric ranging from -1 to 1 that evaluates whether the predicted and true damage maps exhibit similar trends across spatial positions over an image. Therefore, the chosen metrics complement each other to provide a more comprehensive performance assessment. To further examine the surrogate models' capability in capturing local variations in damage intensity across spatial regions, Fig. 6 shows a line-trace comparison between ground truth and predicted damage maps from the K=10 model on the same representative test set sample from the previous figure. The surrogate predictions generally follow the spatial rise-and-fall behavior of the ground truth distributions and capture the locations of major damage peaks for all models. However, highly localized damage regions in the true damage maps appear more smeared in the surrogate predictions and this can also be observed on the line-trace plots where the peak damage intensity value as well as the slope around sharp peaks are underestimated in some cases.

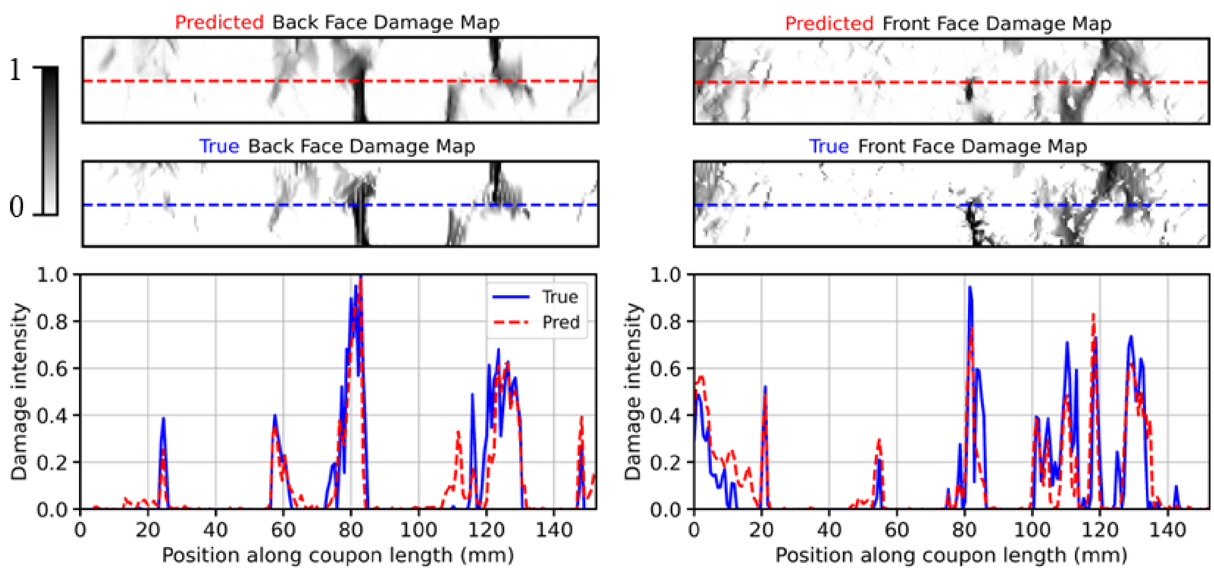

Figure 6. Predicted vs true damage intensity profile along the coupon length

Overall, the results demonstrate the potential of using more accessible, reduced-resolution structural representations for analyzing spatial damage distributions in morphologically complex material systems such as PPMCs.

5. Conclusion

This study examined the extent to which spatial distributions of damage in Prepreg Platelet Molded Composites can be inferred from reduced-resolution structural representations using a data-driven surrogate modeling framework. Through-thickness averaged distributions of second-order orientation tensor components at multiple resolution levels were investigated as deliberately coarsened descriptions of the underlying platelet-scale morphology. The surrogate models successfully identified major damage regions and reproduced distributed damage behavior from reduced structural descriptors. Increasing structural representation resolution improved prediction quality and enabled sharper damage localization behavior to be reproduced. In contrast, progressively coarsened representations resulted in smoother damage field predictions with reduced local detail, while still identifying the locations of major damage sites.

The results indicate that reduced mesoscale structural representations that are coarsened through the thickness dimension retain meaningful information relevant to macroscopic damage evolution in PPMCs. More broadly, the present work demonstrates the potential of data-driven surrogate models not only as approximations of physics-based simulations, but also as tools for investigating the sufficiency of accessible, reduced-resolution structural representations in multiscale analysis of morphologically complex composite systems.

6. References

[1] Kravchenko SG, Sommer DE, Denos BR, Favaloro AJ, Tow CM, Avery WB. “Tensile properties of a stochastic prepreg platelet molded composite,” *Compos. Part Appl. Sci. Manuf.*, vol. 124, p. 105507, Sep. 2019, doi: 10.1016/j.compositesa.2019.105507.

[2] L. Gulfo, O. Haglund Nilsson, J. Sjöberg, I. Katsivalis, L. E. Asp, and M. Fagerström, “A 3D voxel-based mesostructure generator for finite element modelling of tow-based discontinuous composites,” *Compos. Part B Eng.*, vol. 278, p. 111405, Jun. 2024, doi: 10.1016/j.compositesb.2024.111405.

[3] J. Ryatt and M. Ramulu, “Prediction of tensile failure of stochastic tow-based discontinuous composites via mesoscale finite element analysis,” *Compos. Struct.*, vol. 279, p. 114769, Jan. 2022, doi: 10.1016/j.compstruct.2021.114769.

[4] B. R. Denos, D. E. Sommer, A. J. Favaloro, R. B. Pipes, and W. B. Avery, “Fiber orientation measurement from mesoscale CT scans of prepreg platelet molded composites,” *Compos. Part Appl. Sci. Manuf.*, vol. 114, pp. 241–249, Nov. 2018, doi: 10.1016/j.compositesa.2018.08.024.

[5] Y. Wan, I. Straumit, J. Takahashi, and S. V. Lomov, “Micro-CT analysis of internal geometry of chopped carbon fiber tapes reinforced thermoplastics,” *Compos. Part Appl. Sci. Manuf.*, vol. 91, pp. 211–221, Dec. 2016, doi: 10.1016/j.compositesa.2016.10.013.

[6] N. Feld, C. Maeyens, B. Delattre, and N. Grandmaison, “Modelling the effect of process-induced anisotropy on the constitutive behavior of chopped fiber composites,” *Compos. Part Appl. Sci. Manuf.*, vol. 101, pp. 334–343, Oct. 2017, doi: 10.1016/j.compositesa.2017.06.012.

[7] Z. Chen, M. Yacouti, M. Shakiba, J.-X. Wang, T. Luo, and V. Varshney, “Predicting stress and damage in carbon fiber-reinforced composites deformation process using composite U-net surrogate model,” *Theor. Appl. Mech. Lett.*, vol. 16, no. 1, p. 100634, Jan. 2026, doi: 10.1016/j.taml.2025.100634.

[8] A. Gupta, A. Bhaduri, and L. Graham-Brady, “Accelerated multiscale mechanics modeling in a deep learning framework,” *Mech. Mater.*, vol. 184, p. 104709, Sep. 2023, doi: 10.1016/j.mechmat.2023.104709.

[9] Y. Gao, R. Duddu, S. Kolouri, A. Gupta, and P. Prabhakar, “An inverse design framework for optimizing tensile strength of composite materials based on a CNN surrogate for the phase field fracture model,” *Compos. Part Appl. Sci. Manuf.*, vol. 192, p. 108758, May 2025, doi: 10.1016/j.compositesa.2025.108758.

[10] D.-W. Kim, M.-S. Go, J. H. Lim, and S. Lee, “Data-driven stress and strain curves of the unidirectional composites by deep neural networks with principal component analysis and selective-data augmentation,” *Compos. Struct.*, vol. 313, p. 116902, Jun. 2023, doi: 10.1016/j.compstruct.2023.116902.

[11] A. Ani, R. Nakka, G. Subhash, J.-F. Molinari, and S. A. Ponnusami, “Machine learning for computational fracture and damage mechanics— Status and perspectives,” *Eng. Fract. Mech.*, vol. 332, p. 111778, Feb. 2026, doi: 10.1016/j.engfracmech.2025.111778.

[12] *Digimat-FE Software v2024.1*. Hexagon AB.

[13] *Abaqus Standard 2022*. Dassault Systèmes.

[14] D. E. Sommer, S. G. Kravchenko, B. R. Denos, A. J. Favaloro, and R. B. Pipes, “Integrative analysis for prediction of process-induced, orientation-dependent tensile properties in a stochastic prepreg platelet molded composite,” *Compos. Part Appl. Sci. Manuf.*, vol. 130, p. 105759, Mar. 2020, doi: 10.1016/j.compositesa.2019.105759.

[15] S. G. Advani and C. L. Tucker, “The Use of Tensors to Describe and Predict Fiber Orientation in Short Fiber Composites,” *J. Rheol.*, vol. 31, no. 8, pp. 751–784, Nov. 1987, doi: 10.1122/1.549945.